Structure–Property Behavior of Nanofibers Based on Polyacrylonitrile/ Mesoporous Silica (SBA-15) Composites Prepared by Electrospinning

Muhammad Hassan Rafe, Khuram Shahzad, Ludovic Josien, Magali Bonne, Elham Mohsenzadeh, Christelle Delaite, Bénédicte Lebeau, Dominique C Adolphe

Structure–Property Behavior of Nanofibers Based on Polyacrylonitrile/ Mesoporous Silica (SBA-15) Composites Prepared by Electrospinning

Muhammad Hassan Rafe[1,2,3,4] · Khuram Shahzad[8] · Ludovic Josien[2,4] · Magali Bonne[2,4] · Elham Mohsenzadeh[5,6,7] · Christelle Delaite[1,4] · Bénédicte Lebeau[2,4] · Dominique C. Adolphe[3,4]

1 Laboratoire de Photochimie et d'Ingénierie Macromoléculaires (LPIM), Université de Haute-Alsace (UHA), 68100 Mulhouse, France
2 Institut de Science des Matériaux de Mulhouse (IS2M), Université de Haute-Alsace (UHA), CNRS UMR 7361, 68100 Mulhouse, France
3 Laboratoire de Physique et Mécanique Textiles (LPMT), Université de Haute-Alsace (UHA), 68100 Mulhouse, France
4 Université de Strasbourg, 6700 Strasbourg, France
5 GEMTEX, ENSAIT, ULR 2461, 59000 Lille, France
6 Junia, 59000 Lille, France
7 Univ. Lille, 59000 Lille, France
8 Functional Materials Lab, Department of Physics, Air University, Islamabad, Pakistan

Corresponding authors : dominique.adolphe@uha.fr, christelle.delaite@uha.fr, benedicte.lebeau@uha.fr

Abstract
Polyacrylonitrile/mesoporous silica (SBA-15) composites were synthesized using needless electrospinning technique, where, different dispersing agents were examined for better deagglomeration of silica particles in starting formulations and distribution in the electrospun composite nanofibers. Silica nanoparticles increase the specific surface area from 68.7 to 98.5 m^2/g and the tensile strength from 0.61 to 1.22 MPa of PAN nanofibers. Three different dispersing agents including BYK W-9010, BYK W-980 and BYK W-966 were used and the best was optimized for better deagglomeration of silica sub-micron particles in composite nanofibers. PAN composite nanofibers also increased thermal stability up to 650 °C than pristine PAN nanofibers due to hydrogen bridges present between nitrile groups of PAN and silanol groups of fillers.

Keywords Polyacrylonitrile · Ordered mesoporous silica · SBA-15 · Dispersing agent · Electrospinning

1 Introduction

Nanotechnology has a large impact in manufactured products in most major industry sectors, including electronics, cosmetics, automotive and healthcare sectors [1–5]. According to recent survey, over 1300 nanotechnology related products are currently in the market [6–9]. Nanofibers can be produced by different methods, such as jet blowing, melt blowing, co-extrusion, interfacial polymerization and electrospinning [10, 11]. Electrospinning is a versatile and simple technique that is used to produce very fine homogeneous micro- or nanofibers [12, 13]. One unique feature of electrospinning is its capability to control the fibers diameter (from tens of nanometers to a few micrometers) by varying processing parameters, such as starting formulation composition, applied voltage, fluid flow rate, tips to collector distance and precursor solution viscosity. This control of fibers diameter makes the nanofibers suitable for different applications [14–16]. The produced electrospun nanofibers have high porosity and high surface area to volume ratio. These properties contribute a lot in potential applications such as manufacturing of carbon and graphitic nanofibers, tissue scaffolding, drug delivery systems, filtration and reinforced nanocomposites [2, 17, 18]. PAN has been selected in this study for electrospun nanofibers for two reasons: (1) PAN has been widely used for ultrafiltration, nanofiltration and reverse osmosis due to its good solvent resistance and, (2) PAN has also been electrospun into precursor form to fabricate carbon nanofibers [12]. Electrospun PAN nanofibers have attracted considerable attention in the field of water filtration as they exhibit a number of unique features including large surface area with enough mechanical strength and good chemical resistance [6]. For the process of electrospinning, a suitable solvent has to be found to dissolve the desired polymers. The suitable solvent should be non-toxic, non-corrosive and environment friendly [19]. Due to these reasons, we selected dimethyl sulphoxide (DMSO) as environment friendly and highly polar solvent to dissolve PAN [20, 21]. Electrospinning is a well-adapted technique to produce polymer-based composites nanofilaments by incorporating fillers in the starting formulation. Several organic or inorganic fillers have been introduced in electrospun polymeric nanofibers to improve functionality and properties of the nanofibers. For example, the incorporation of nanocarbons and nanocellulose has been studied as reinforcement fillers. Silica SBA-15 particles are mesoporous silica materials with a highly ordered two-dimensional hexagonal mesostructure and thick uniform amorphous silica walls

delimiting mesopores with a regular size. They possess a large specific surface area, high pore volume, controllable and narrowly distributed pore sizes, and a high density of silanol groups (SiOH) are distributed over the silica surface [22, 23]. The interest in these materials in several applications such as drug delivery systems, catalysis, sensors, and adsorption that benefit of the properties of these materials is growing [24, 25]. The combination of mesoporous silica and electrospun polymer nanofibers leads to composite that offer the best of both components [26]. The dispersion of the silica nanoparticles in the polymer solution prior to the electrospinning process is necessary in order to produce smooth nanofibers. Indeed, silica particles usually tend to agglomerate by Van der Waal's forces and hydrogen bonds. Dispersion of silica nanoparticles with a dispersing agent results the modification of their surface energy, which prevents the reagglomeration of SBA-15 particles [22, 27]. There are some limitations in the work; at time of research it was not possible to perform experiments on all samples for application. However, the present study deals with the adjustment of the PAN concentrations in DMSO and optimization of the electrospinning parameters to produce electrospun PAN nanofibers. The effect of incorporating SBA-15 particles with and without a dispersing agent on the properties of the produced electrospun composite PAN/SBA-15 nanofibers will be described.

2 Experimental

2.1 Materials

Polyacrylonitrile (PAN) with Mw _ 150,000 g/mol and DMSO (99.9% pure) were purchased from Sigma-Aldrich. SBA-15 silica particles have been synthesized according to Y. Belmoujahid et al. procedure [28]. Dispersing agents (DA) of W-9010, W-966 and W-980 (99.96%) were provided by BYK Company (Germany). A few specifications of all used dispersing agents are mentioned below in Table 1.

Table 1 Specifications of dispersing agents used in this study

Specifications	BYK W-9010	BYK W-980	BYK W-966
Acid Value (KOH/g)	129	40	26
Density (20 °C, g/ml)	1.16	0.99	0.87
Refractive Index (20 °C)	1.469	1.32	1.263
Recommended value (%)	0.5–1	0.5–1.5	0.5–1.5

2.2 Synthesis of SBA-15

First, 3.5 g of porogen agent Pluronic P123 (99% pure Sigma- Aldrich) was dissolved in 16.5 mL of HCl (12M) (Riedel de Haen 37 wt. %) and 112 mL of distilled water. The solution was heated at 40 °C and maintained under vigorous stirring until complete dissolution of P123. Second, 7.427 g of tetraethoxysilane (TEOS 99.9%, Sigma-Aldrich) the silica precursor was then rapidly added to P123 acidic solution. After ripening at 40 °C for 2 h without stirring, the mixture was transferred to an oven for further silica condensation at 90 °C under static conditions for 24 h. Finally, the product was recovered by filtration, washed with distilled water until neutral pH, dried at 70 °C and calcined at 300 °C under air for 4 h to liberate the porosity occluded by the P123. The obtained SBA-15 sub-micron particles have a length ranges from 1 to 2 μm and a width ranges from 400 to 500 nm.

2.3 Selection of the Dispersing Agent

The best dispersing agent was selected by measuring the particle size of SBA-15 suspended in DMSO with 1 wt% compared to the weight of SBA-15 particles. The optimal amount of the selected dispersing agent was also determined from particle size measurements of SBA-15/DMSO formulations containing from 0.5 to 2 wt% of dispersing agent.

2.4 Preparation of PAN-Based Formulations for Electrospinning

PAN/DMSO solutions with or without dispersing agent and SBA-15 were prepared at different PAN concentrations in DMSO (X = from 5 to 12 wt %) for a rheological study in order to identify the better concentration in term of viscosity for electrospinning process. For all SBA-15-containing formulations, the PAN/SBA-15 weight ratio was fixed to5.PAN/DMSO formulations are: Xwt% PAN, Xwt% PAN/(5:1 PAN/SBA-15 wt ratio)SBA-15 and Xwt%PAN/(5:1 PAN/SBA-15 wt ratio)SBA-15/(1 wt% dispersing agent compared to SBA-15). Each SBA-15 containing suspension was stirred for 40 min by IKA® T18 digital Ultra Turrax to make the suspension homogeneous with well deagglomeration of SBA-15particles. The formulations were further stirred at room temperature with magnetic stirrer at 300 r.p.m for one day to make the mixtures stable and were stirred again for 15 min with Ultra Turrax at 1000 r.p.m just before electrospinning.

2.5 Electrospinning of PAN-Based Formulations

For electrospinning, a needleless electrospinning machine "Nanospider Lab" (Elmarco, Czech Republic) was used. The electrospinning parameters such as voltage, electrode substrate distance, nozzle diameter (for feeding the solution) and carriage speed (which controls the speed of wire) were varied to find optimum conditions. The relative humidity was kept at 33 ± 2 %, and the room temperature was 20 ± 2 °C.

2.6 Characterization

2.6.1 Viscosity Measurements

The viscosity of PAN formulations in DMSO was measured by using Anton Paar Modular Compact Rheometer 502 on "plan-plan mode" at 20 °C. The formulations are prepared by using Ultra Turrax homogenizer at 1000 r.p.m. for 40min and magnetic stirrer for one day to make them homogeneous at ambient temperature. Just before viscosity measurement the formulation was stirred again for 15 min with Ultra Turrax homogenizer. An average value of viscosity was determined from five measurements realized on each formulation.

2.6.2 Particle Size Measurements

The sizes of SBA-15 particles with and without BYK (from 0.5 to 2 wt% compared to SBA-15) were determined by light scattering using a ZETASIZER nanoseries (by Malvern company) in DMSO. Prior to analysis, each suspension was stirred with Ultra Turrax homogenizer at 1000 r.p.m for 20 min. An average value of particle size was determined from the measurements realized on three identical formulations.

2.6.3 Morphology and Surface Topology

The morphology and surface topology of nanofibers were examined by using Scanning Electron Microscopy (SEM) JEOL JSM-IT100. Hundred measurements were carried out on each sample by Image J 1.45S software to obtain the average nanofibers diameter.

2.6.4 Tensile Strength Tests

Tensile strength tests of all nanofibers, including raw PAN, PAN composite nanofibers with and without dispersing agents having dimensions of 40 × 20 mm^2 were performed on MTSM/20 tensile testing machine at 20 ± 2 °C and 65 ± 2% relative humidity. The distance between sample holding jaws was 20 mm and speed of jaws was 20 mm/min. Five samples of each nanofibers membrane were tested to get an average value of both tensile strength and Young modulus.

2.6.5 Thermogravimetric Analysis (TGA)

Thermogravimetric analysis (TGA) of pure PAN nanofibers and composite PAN nanofibers was performed on a TGA Q500 machine at room temperature and pressure. The temperature profile for thermal analysis of samples was set from 25 to 800 ^oC at the increasing rate of 10 °C/min.

2.6.6 Textural Properties

The textural properties of SBA-15 and electrospun composite PAN nanofibers were characterized by nitrogen adsorption/desorption analysis that was performed on a Tristar apparatus (Micrometrics) at -196 °C. Before the measurements, all samples of silica nanoparticles and composite nanofibers were out gassed in vacuum at 150 °C for 20 h under the pressure of 1.33 Pa. This process of degassing results in removal of physisorbed water avoiding silica dehydroxylation. The specific surface area and the pore diameter of SBA-15 particles and composite nanofibers were determined by BET (Brunauer–Emmett–teller) method and BJH (Barrett-Joyner-Halenda) model applied on the desorption branch, respectively [29, 30]. The total pore volume was calculated at $p/p^\circ = 0.9$.

3 Results and Discussion

3.1 Effect of the Dispersing Agent on the Deagglomeration of SBA-15 Particles in DMSO

Three dispersing agents of BYK W-9010, BYK W-966 and BYKW-980 were used to check their efficiency to deagglomerate SBA-15 particles in DMSO. For this purpose, three formulations of 2wt% of SBA-15 in DMSO were prepared and 0.5, 1, 1.5 and 2wt% of each dispersing agent compared to SBA-15 was added in the suspension, respectively. As reference, a suspension of SBA-15 without dispersing agent in DMSO was also prepared. The data reported in Table 2 presents the mean values of particles size measured by light scattering measurements were done on 3 identical formulations for each composition.

Table 2 Average SBA-15 particles size suspended in DMSO with and without dispersing agents

S. No	Sample Name	Size (nm)
1	SBA-15	596 ± 45
2	SBA-15 + 0.5 wt% BYK W-9010	632 ± 98
3	SBA-15 + 0.5 wt% BYK W-980	562 ± 70
4	SBA-15 + 0.5 wt% BYK W-966	561 ± 70
5	**SBA-15 + 1 wt% BYK W-9010**	**120 ± 18**
6	**SBA-15 + 1 wt% BYK W-980**	**326 ± 35**
7	**SBA-15 + 1 wt% BYK W-966**	**337 ± 48**
8	SBA-15 + 1.5 wt% BYK W-9010	301 ± 36
9	SBA-15 + 1.5 wt% BYK W-980	300 ± 35
10	SBA-15 + 1.5 wt% BYK W-966	310 ± 41
11	SBA-15 + 2 wt% BYK W-9010	383 ± 55
12	SBA-15 + 2wt% BYK W-980	333 ± 44
13	SBA-15 + 2wt% BYK W-966	417 ± 52

The larger particles sizes of 596 nm were observed for SBA-15/DMSO suspension without dispersing agent highlighting the agglomeration of the particles. In presence of the dispersing agents smaller particle sizes are observed, revealing a lowdisparity in particle size. The smallest particle size of 120 nm is reached with 1 wt% of BYK W-9010indicating that this is the most effective additive to deagglomerate the silica nanoparticles. The particles sizes of SBA-15 formulations in DMSO with different BYKW-9010 concentrations from 0.5 to 2 wt% were measured to optimize the amount of dispersing agent (Table 2). With 0.5 wt% of dispersing agent the particle size is as high as for SBA- 15/DMSO suspension without dispersing agent indicating that the amount of dispersing agent is too low to deagglomerate SBA-15 particles. According to the results the lowest particle size was measured for 1 wt% of BYK W-9010. The dispersing agent causes deagglomeration of silica particles in the solution by coating the surface of the inorganic filler, which creates steric repulsion between the particles.

3.2 Effect of PAN Concentration on Formulation Viscosity

The average viscosities of the DMSO formulations of PAN from 5 to 12 wt% concentrations with PAN: SBA-15 of 5:1 wt:wt ratios of SBA-15 are reported in Fig. 1. The results show that increasing the concentration of PAN in DMSO increases the viscosity. The increase in viscosity is ascribed to the increase of attractive forces between positive and negative components within a molecule and increase in the volume of polymer coil in the solution [20]. In the same way, dispersion forces, stronger polarization and hydrogen bonding between the solvent and the polymer affects the viscosity [20].

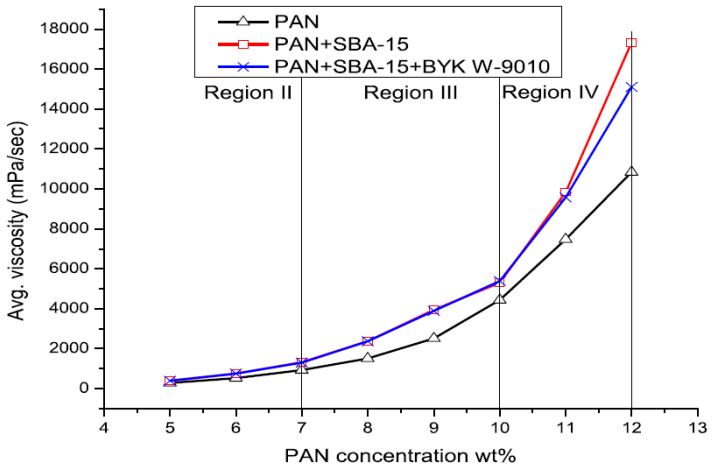

Fig. 1 Average viscosities of PAN formulations at different concentrations in DMSO without and with SBA-15 (5:1 wt) and SBA-15 + BYK W-9010

As it is demonstrated in Fig. 1, incorporating SBA-15 increases the viscosity and addition of BYK dispersing agent has no effect on the viscosity. From previous studies, it has been concluded that there are four regimes of specific viscosity [31]. Regime I (not observed) is diluted regime where viscosity is very low so usually 1-2wt% of polymer solutions fall in this range. The regime II corresponds to semi-dilute unentangled regime where viscosity is higher than the ones of the regime I but not high enough for electrospinning since polymer chains will not entangle to each other to make nanofibers: from 5 to7 wt% of PAN, polymer solutions are considered in this range. The regime III corresponds to semi-dilute entangled regime where there is enough entanglement of polymer chains for electrospinning. In this study, the specific viscosity values of 8wt% and 10wt% of PAN fall in these regime favorable or good electrospun nanofibers. Whereas the regime IV (above 10 wt% of PAN) is concentrated regime whose viscosity is quite higher than all other regimes [31]. Therefore, in this study for electrospinning of smooth nanofibers, 8wt% and 10wt% of PAN concentrations were selected. The formulations of PAN suitable for electrospinning and their viscosities, taken from Fig. 1, are summarized in Table 3. The viscosity of the solution has a great impact on the electrospinnability and on the morphology of the resulting nanofibers [31]. The viscosity of polymer solution profoundly influences the jet formation and jet stability and is crucial for the successful formation of smooth nanofibers. The solution has to maintain appropriate viscosity in order to survive stretching, acceleration and whipping [32, 33]. In Table 2, specific viscosities of the solutions are also mentioned. Specific viscosity is the incremental viscosity of the solution due to the presence of polymer. It is measured by using Eq. 1:

$$\eta_{sp} = (\eta - \eta_0)/\eta_0 \qquad (1)$$

where η is the viscosity of solution and η_0 is the viscosity of solvent.

Table 3 Suitable Viscosities of PAN formulations for electrospinning

Sr. No	Sample name	Viscosity* (mPa/sec)	Specific viscosity (mPa/sec)
1	8wt% PAN	1516 ± 63	757 ± 32
2	10wt% PAN	4442 ± 27	2220 ± 13
3	8wt% PAN + 1.7wt% SBA-15	2380 ± 35	1189 ± 17
4	10wt% PAN + 2wt% SBA-15	5302 ± 44	2650 ± 22
5	8wt% PAN + 1.7wt% SBA-15 + 0.017**wt% BYK W-9010	2370 ± 53	1184 ± 26
6	10wt% PAN + 2wt% SBA-15 + 0.02**wt% BYK W-9010	5390 ± 43	2694 ± 21

**Average values from five measurements*
*** 0.02 and 0.017wt% of BYK W-9010 in the formulations. These values correspond to 1wt% compared to SBA-15*

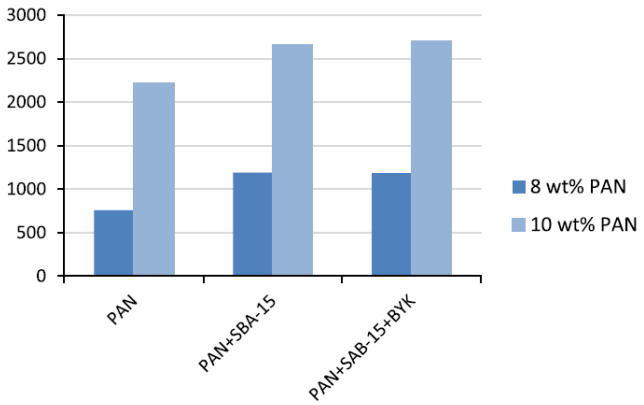

Fig. 2 Specific viscosity of 8 and 10 wt% PAN/DMSO formulations

Specific viscosity expresses the incremental viscosity due to the presence of the polymer in the solution. The graphical form of specific viscosity is shown in Fig. 2. Regardless of the formulation composition, the specific

viscosity is more than twice higher for 10wt% PAN formulations compared to 8 wt% ones. Higher increase of viscosities can be attributed to semi-dilute entangled regime (Region III). The addition of polymer contributes mainly in entanglements of polymer chains resulting in higher viscosity. For both 8 and 10wt% PAN-based formulations the specific viscosity increases with SBA-15 and with SBA-15 + BYK W-9010. However, there is no difference between PAN/SBA- 15 and PAN/SBA-15 + BYKW-9010. The specific viscosity is mainly impacted by the presence of the SBA-15 in the formulations.

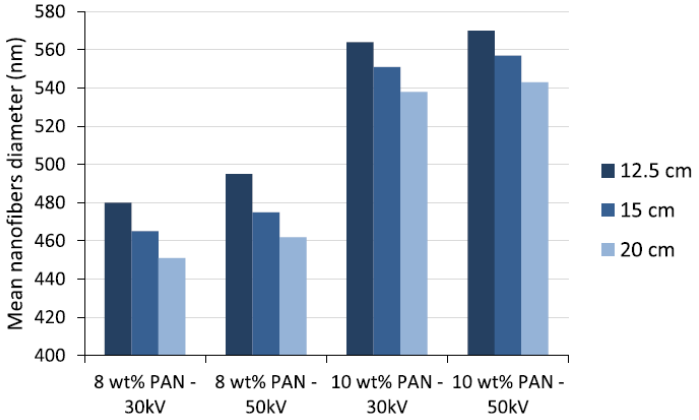

Fig. 3 Variation of the average diameter of PAN nanofibers with voltage and electrode distance

3.3 Nanofibers Diameter

For all formulations of PAN, PAN/SBA-15 and PAN/SBA- 15/BYK W-9010 in DMSO the electrospinning parameters were electrode voltage of 30and 50 kV, electrode distance of 12.5, 15and 20 cm and feed nozzle size of 0.8 mm. For each sample, the electrospinning duration was 15 min. The tested electrospinning parameters and resulting nanofibers diameter (determined by SEM in Fig. 4, from hundred measurements realized on each sample by J image software) with coefficient of variation (CV %) are reported in Table 4.

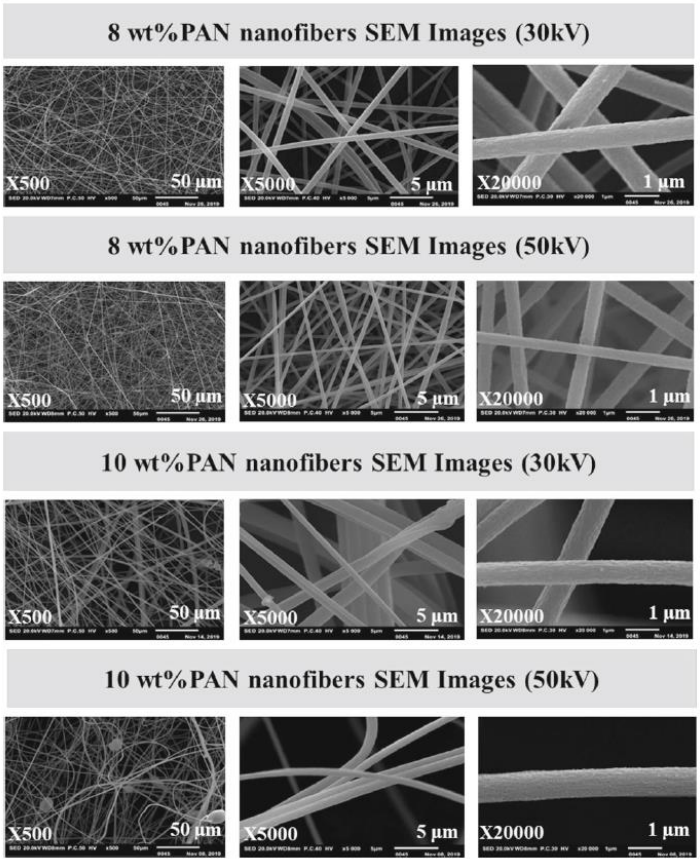

Fig. 4 SEM images of raw PAN nanofibers (electrode distance = 15 cm)

Table 4 Electrospinning parameters and average diameters of nanofibers produced from 8 and 10 wt% PAN formulations

S.No	Sample name	Voltage (kV)	Distance (cm)	Nanofibers diameter (nm)-Standard deviation CV in %
1	PAN 8wt%	30	12.5	480 ± 46–CV% = 10
2			15	465 ± 55–CV% = 12
3			20	451 ± 56–CV% = 12
4		50	12.5	495 ± 54–CV% = 11
5			15	475 ± 50–CV% = 11
6			20	462 ± 55–CV% = 12
7	PAN 8wt% + 1.7wt%* SBA-15	30	12.5	585 ± 123–CV% = 21
8			15	577 ± 103–CV% = 18
9			20	561 ± 87–CV% = 15
10		50	12.5	587 ± 78–CV% = 13
11			15	573 ± 73–CV% = 12
12			20	552 ± 74–CV% = 14
13	PAN 8wt% + 1.7wt%* SBA-15 + 0.017wt%**BYKW9010	30	12.5	548 ± 49–CV% = 9
14			15	560 ± 51–CV% = 9
15			20	533 ± 47–CV% = 9
16		50	12.5	575 ± 49–CV% = 8.5
17			15	534 ± 47–CV% = 9
18			20	513 ± 50–CV% = 10
19	PAN 10wt%	30	12.5	564 ± 53 CV% = 9
20			15	551 ± 57 CV% = 10
21			20	538 ± 49 CV% = 9
22		50	12.5	570 ± 56 CV% = 10
23			15	557 ± 51–CV% = 9
24			20	543 ± 49–CV% = 9
25	PAN10 wt% + 2wt%* SBA-15	30	12.5	669 ± 78–CV% = 12
26			15	652 ± 78–CV% = 12
27			20	646 ± 73–CV% = 11
28		50	12.5	668 ± 79–CV% = 12
29			15	651 ± 77–CV% = 12
30			20	638 ± 67–CV% = 11
31	PAN 10wt% + 2wt%* SBA-15 + 0.02wt%**BYKW9010	30	12.5	652 ± 59–CV% =9
32			15	645 ± 58–CV% = 9
33			20	634 ± 60–CV% = 9
34		50	12.5	655 ± 57–CV% = 9
35			15	644 ± 58–CV% = 9
36			20	640 ± 53–CV% = 8

** wt% compared to PAN and corresponding to 5:1 wt ratio of PAN: SBA-15*

*** 0.02 and 0.017wt% of BYK W-9010 in the formulations correspond to 1wt% compared to SBA-15*

3.3.1 Raw PAN Nanofibers

The variation of the average diameter of PAN nanofibers with electrode distance produced from 8wt%PANand 10wt%PAN solutions at 30 and 50 kV is displayed in Fig. 3. Whether the voltage is, 30 or 50 kV, for a given PAN concentration, the diameter of nanofibers decreases with the increase of the electrode distance. The reason behind is that longer collecting distance offers a longer flight time for the jet so the jet is stretched further and there is enough time available for solvent to evaporate, thus finer fibers are produced [34, 35]. Nevertheless, this variation is weak since it is in the error domain. Table 5 describes that by increasing electrode distance, diameter of nanofibers is decreased by keeping polymer concentration and applied voltage constant. By increasing the voltage from 30 to 50 kV, the diameter of nanofibers increased, which is due to the flight time of the jet. Indeed, higher voltage will accelerate the jet and reduce the flight time. Shorter flight time will offer less time for fibers to be stretched and elongated [36]. Synergistically, higher voltage may accelerate the solvent evaporation rate. However, the impact of the PAN concentration on the nanofiber's diameter is important (about 100 nm) highlighting the role of the viscosity on the nanofibers diameter. The reason is that by increasing the polymer concentration, viscosity increased as a result of the increase of the number of polymer chain entanglements and thus the viscoelastic forces. SEM images of raw PAN nanofibers with the best standard deviation (SD) and coefficient of variation (CV %) are displayed in Fig. 4.

Table 5 Effect of nanofibers diameter by varying the electrode Distance

Sample name	Voltage (Kv)	Electrode distance		
		12.5 cm	15 cm	20 cm
8wt% PAN	30	480 nm	465 nm	451 nm
	50	495 nm	475 nm	462 nm
10wt% PAN	30	564 nm	551 nm	538 nm
	50	570 nm	557 nm	543 nm

In all cases, PAN nanofibers have smooth surface and look quite homogeneous in diameter. However, a close look of nanofibers obtained at 50 kV reveals the presence of some bulbs, especially in the case of the 10wt%electrospunPANwith electrode distance of 15 cm (below left).

3.3.2 PAN Composite Nanofibers

In this section, the morphology of PAN and PAN/SBA-15 composite nanofibers with and without dispersing agent are discussed. The variation of the nanofibers diameter at 30 kV with electrode distance for the 8 and 10wt% PAN formulations containing SBA-15 and in presence or not of dispersing agent is displayed in Fig. 5. By adding SBA-15 particles, the diameter of nanofibers is increased whatever the PAN concentration. Adding dispersing agent in composite nanofibers reduces the diameter of nanofibers and CV% compared to PAN/SBA-15 nanofibers as a result of a better deagglomeration of silica nanoparticles.

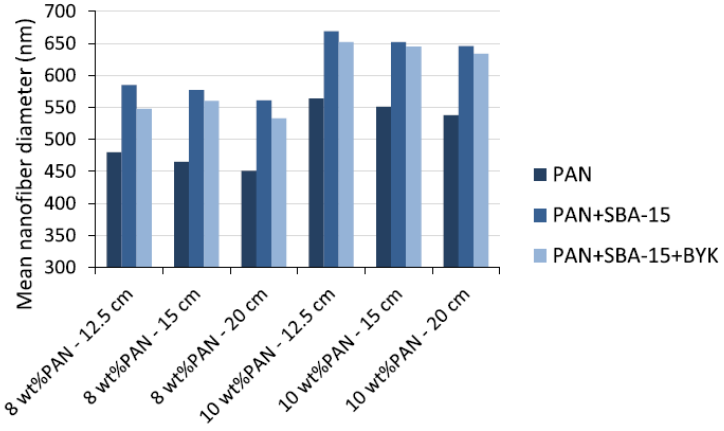

Fig. 5 Variation of diameter at 30 kV and different electrode distances of PAN and PAN composite nanofibers formulations (8 wt % and 10 wt %) with SBA-15 and with SBA-15 + BYKW-9010

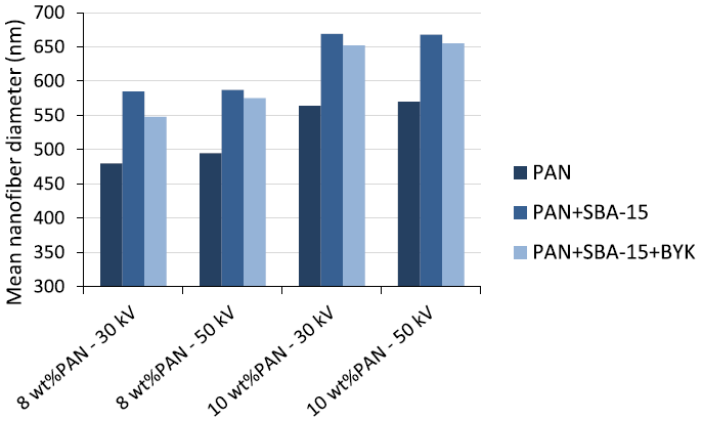

Fig. 6 Effect of voltage at fixed electrode distance of 12.5 cm on thediameter of PAN and PAN composite nanofibers concentrations of 8 and 10 wt % with SBA-15 and with SBA-15 + BYKW-9010

The increase in PAN concentration from 8to 10wt% and thus SBA-15 concentration (from 1.7wt% of SBA-15 in each 8wt% of PAN formulation to 2wt%of SBA-15 in each 10wt%of PAN formulation) increased the diameter of nanofibers due to the increase of solution viscosity indicating a better entanglement of polymer chains [36]. In most of the cases, by increasing electrode distance, the diameter of nanofibers slightly decreased due to extra time

of flight jet that resulted in more extension of polymer jet and more time of jet relaxation. Figure 6 illustrates the effect of the voltage that was varied from 30 to 50 kV on the nanofibers diameter. For 8wt % PAN formulations, the nanofibers diameter in most of the cases is slightly increased with the increase of the voltage because the high electrolytic force [36] reduces the flight time of polymer jet and increases the evaporation of the solvent. However, for 10 wt% PAN the nanofibers diameter remained almost constant by increasing voltage. In Fig. 7, a selection of SEM images of composite nanofibers with and without dispersing agent are displayed with standard deviation (SD) and coefficient of variation (CV%) values.

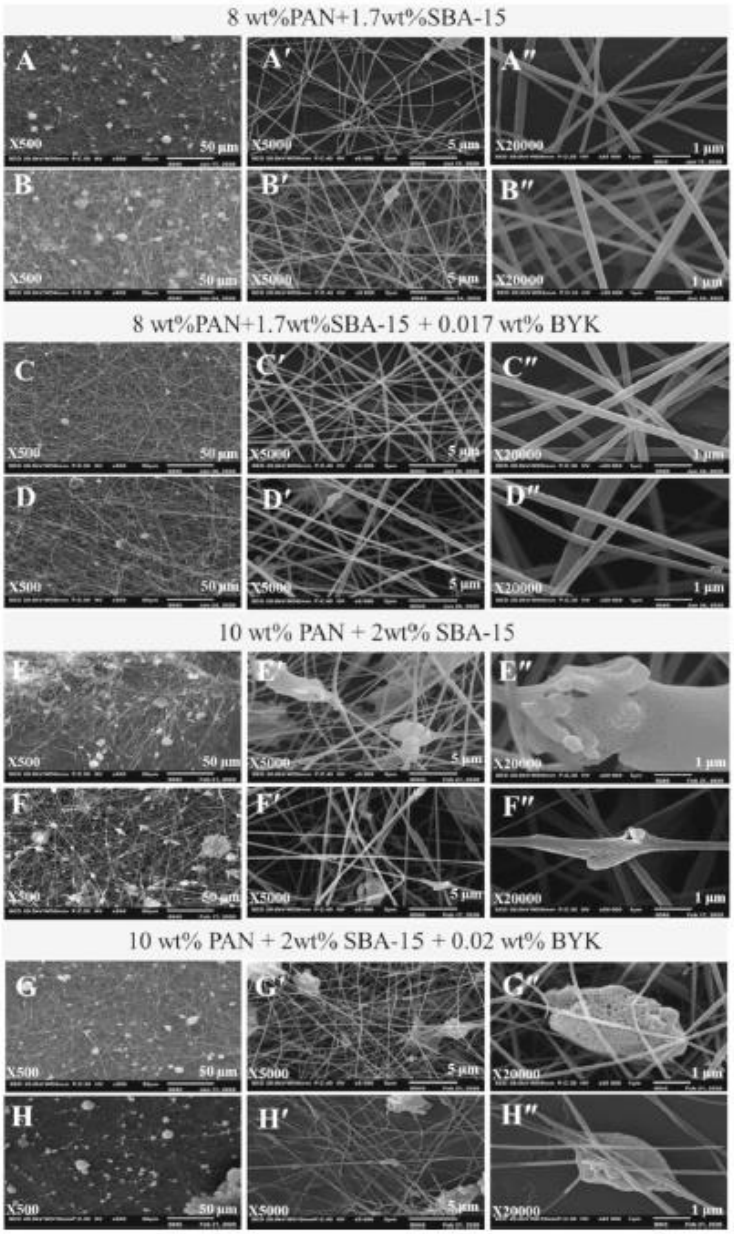

Fig. 7 SEM images of PAN/SBA-15 composite nanofibers produced at 30 and 50 kV (Electrode distance _ 12.5 cm)

For 8 wt % PAN/PAN + SBA-15 formulations, there is no noticeable change in the nanofibers diameter by increasing the voltage, however, the nanofibers diameter of PAN+ SBA-15 +BYK is slightly increased with the increase of the voltage, regardless of composition. This is because the high electrolytic force will reduce the flight time of polymer jet and increases the evaporation of the solvent [36]. In Fig. 7, a selection of SEM images of composite nanofibers with and without dispersing agent are displayed with standard deviation (SD) and coefficient of variation (CV%) values. Whether the PAN concentration is 8 or 10 wt%, for both high voltages 30 and 50 kV, at low magnification, PAN/SBA- 15 nanofibers are coexisting with several aggregates that appear sticked to the nanofibers. EDX coupled SEM analyses were realized and confirmed that these aggregates were made of raw PAN

(See EDX C and N elemental mappings displayed in Fig. S1). At higher voltage (50 kV) the aggregates appear more numerous and/or bigger (Fig. 7A, B, E, F). At high magnification, the presence of rod-shape SBA-15 particles is observed as isolated and glued in nanofibers or glued in the aggregates (Fig. 7B', E', E', F', F"). The presence of silica particles in the PAN nanofibers and aggregates was confirmed by EDX coupled SEM analyses (See EDX C and N elemental mappings displayed in Fig. S1). Whatever the voltage, for both 8 and 10 wt% PAN concentrations, the addition of dispersing agent appears to decrease the presence of aggregates (Fig. 7C, D, G, H). However, the effect of deagglomeration in the presence of dispersing agent appears more beneficial with 8wt% of PAN.A voltage of 30 kV and a PAN concentration of 8wt% appear the most suitable conditions to produce PAN/SBA-15 composite nanofibers.

3.4 Tensile Strength of Nanofibers

Five tensile tests were performed on each 8 wt% PAN-based nanofibers sample produced at 50 kV and the average tensile strength and Young's modulus are reported in Table 6. The results show that the addition of SBA-15 particles in PAN nanofibers increased the tensile strength compared to raw PAN nanofibers. However, the deagglomeration of SBA-15 particles with dispersing agent did not improve tensile strength as much as did agglomerated SBA-15 particles. High strength of PAN/SBA-15 composite nanofibers with or without dispersing agent is due to interfacial interaction between silica particles and PAN matrix [37].

3.5 Thermogravimetric Analysis (TGA)

To study the thermal degradation of pure PAN nanofibers and PAN/SBA-15 composite nanofibers the process of TGA is commonly used. This process offers a quantifiable analysis of the amount of moisture and volatile compounds present in the nanocomposite fibers, weight loss and thermal breakdown. It is determined that by thermal degradation of polyacrylonitrile: Hydrogen cyanide and ammonia are the main constituents of degradation [38].

Table 6 Tensile strength and Young's Modulus of samples obtained from 8 wt % PAN formulations at 50 kV with electrode distance of 15 cm

S. No	Sample name	Avg. tensile strength (MPa)	Young's modulus E (MPa)
1	8wt% PAN	0.61 ± 0.05	0.06 ± 0.004
2	8wt% PAN+1.7 wt%SBA-15	1.22 ± 0.05	0.12 ± 0.007
3	8wt% PAN+1.7wt%SBA-15 + 0.017 wt%BYK W-9010	0.92 ± 0.08	0.09 ± 0.006

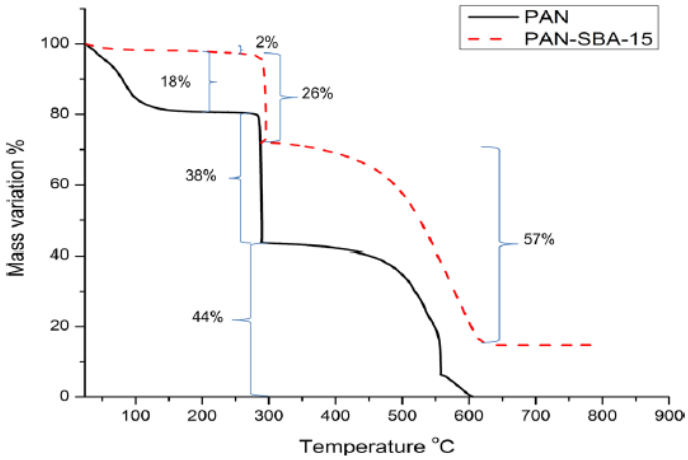

Fig. 8 TGA thermograms of pure PAN (8 wt%) nanofibers and PAN (8 wt%) nanofibers/ SBA-15 (1.7wt %) composites

Figure 8 shows the thermogravimetric curves recorded under air of pure PAN nanofibers and PAN/SBA-15 composite nanofibers.

The heating of PAN produces chemical reactions, such as, cyclization, degradation and cross-linking, so the mechanism of these processes depends on the heating rate, atmosphere, mass of polymer and nature of the filler materials [39]. TGA curves of pure PAN nanofibers and PAN/SBA-15 composite nanofibers show a three-step weight loss. From 20 to 200 °C, both pristine PAN and composite PAN/SBA-15 nanofibers

exhibits a weight loss, which can be attributed to the desorption of DMSO and physically adsorbed water [40]. The major weight loss observed from 250 to 350 °C corresponds to pyrolytic reactions that are exothermic with

maxima at 282 °C for pure PAN nanofibers and at 293 °C for PAN/SBA- 15 composite nanofibers. The pyrolytic reactions correspond to the PAN cyclization reaction [41, 42]. The corresponding weight losses associated to these pyrolytic reactions are 36 and 22% for PAN and PAN/SBA-15 composite nanofibers, respectively. These exothermic weight losses are due to the oligomerization of nitrile groups in PAN [6]. The third weight loss observed in the temperature range from 300 to 650 °C for both pristine PAN and PAN composite nanofibers may be attributed due to the evaporation of anhydrous ammonia(NH_3), (HCN), and PAN polymer chain fragments. The thermal decomposition of pristine PAN is complete at 650 °C but in the case of composite nanofibers, about 20 wt % of residue is remaining at temperature up to 650 °C, which corresponds to SBA-15. Higher thermal stability is observed due to the presence of SBA-15 in pristine PAN nanofibers. The
delay in PAN cyclization is likely due to the strong hydrogen bridges between PAN nitrile groups (–C≡N) and SBA-15 silanol groups (–Si–OH) [6].
TGA and DTA were also realized on PAN/SBA-15/BYK W-9010 composite nanofibers and similar curves were obtained (Fig. S2). From TGA total weight losses; the SBA- 15 contents of 15.7 wt% and 16.7 wt% were determined for 8 wt % PAN/1.7 wt % SBA-15 and 8 wt % PAN/1.7 wt % SBA-15/0.017 wt % BYK nanofibers, respectively.

3.6 N_2 Adsorption/Desorption Measurements

N_2 adsorption/desorption isotherms with BJH desorption pore size distribution of silica SBA-15 and electrospun8 wt% PAN-based composite nanofibers are displayed in Fig. 9.

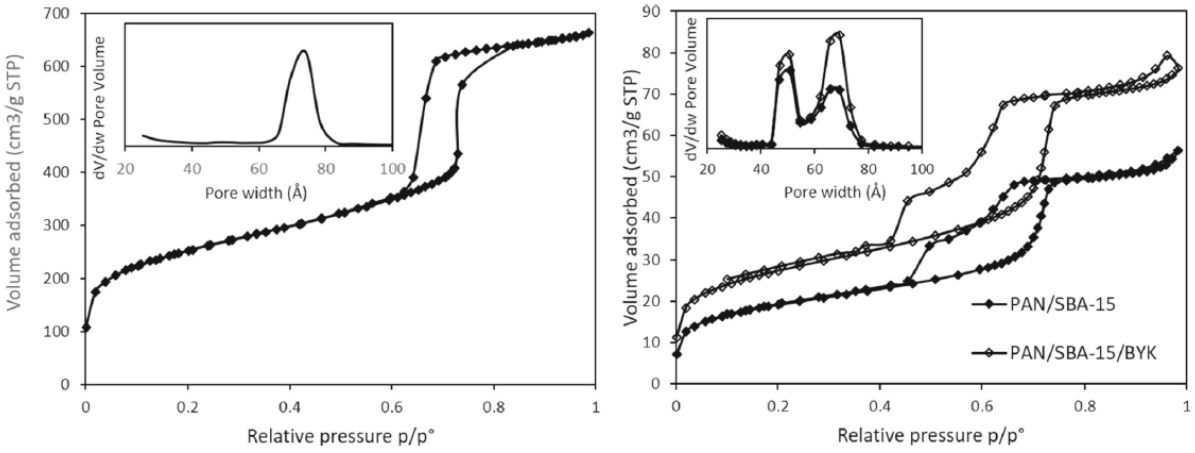

Fig. 9 N_2 adsorption/desorption isotherms of raw SBA-15 (left) and 8 wt % PAN/SBA-15 composites (right). Insets: BJH desorption pore size distributions

The N_2 adsorption/desorption isotherm of raw SBA-15 is a mixture of type I and type IV with an H1-type hysteresis loop according to IUPAC classification [43]. Type I at low relative pressure indicates the presence of micropores. The type IV with a capillary condensation step is characteristic of mesoporous solids. Indeed, SBA-15 silica is characterized by the presence of mesopores arranged in an ordered hexagonal array (about 7 nm of diameter) connected through micropores (V_{micro} _ 0.164 cm^3/g). In H1 type hysteresis loop the adsorption and desorption branches are parallel and quasi-vertical: It is characteristic of capillary condensation and evaporation process in the cylindrical pore open at both ends and these are observed with adsorbents that have a very narrow size distribution of cylindrical mesopores. This is confirmed with the monomodal pore size distribution
(PSD) plot with mesopore diameter of SBA-15 particles in the range of 6.5–8 nm and a maximum at 7 nm. The isotherms of PAN/SBA-15 with and without BYK W-9010 dispersing agent are also a mixture of type I and type IV. There is also a small increase of the volume adsorbed at high relative pressure indicating textural porosity. However, the hysteresis type H1 + H3 is composite and the isotherm looks like the one of plugged hexagonal templated silica (PHTS) material with combined micro- and mesopores. The desorption at higher pressures is associated with the evaporation of liquid from open pores. On the other hand, plugged mesopores remain filled until they empty via cavitation. Consequently, the pore size distribution is bimodal with 2 pore sizes: a small one of about 5 nm due to the cavitation phenomena when plugged mesopores empty, and the larger one of 6.9 nm corresponding to the main mesopores of the raw SBA-15. Pore plugging may be due to the penetration of PAN at the entrance of mesopores. Specific surface areas, pore volumes and pore sizes determined from the N_2 adsorption/desorption isotherms are reported in Table 7.

Table 7 SiO_2 content (wt %) determined by TGA and textural characteristics determined from N_2 adsorption/desorption isotherms

Sample	wt% SiO_2[a]	S_{BET} (m^2/g)	Pore volume[b] (cm^3/g)	Micropore volume[c] (cm^3/g)	Pore width[d] (nm)
SBA-15	100	917	1.02	0.163	5.6
8wt%PAN/1.7 wt% SBA-15	15.7	68.7	0.08	0.009	5.4
8wt%PAN/1.7 wt% SBA-15/0.017 wt% BYK W-9010	16.7	98.5	0.11	0.015	5.5

[a]*weight percentage of SiO_2 in composite nanofibers determined by TGA analysis performed under air = mass loss between 200 and 700 °C*
[b]*determined at p/p0 = 0.9*
[c]*determined by t-plot method*
[d]*value corresponding to the maximum of the PSD*

The specific surface area and pore volumes of composite nanofiber are much smaller than the one of the raw SBA-15 because of the presence of non-porous PAN (83.3 wt% for PAN: SBA-15 wt ratio of 5:1). The TGA realized on composite nanofibers have shown that composite nanofibers without and with BYK W-9010 contain 15.7 wt% and 16.7 wt% of SBA-15, respectively. Since the S_{BET} of raw SBA-15 is 917 m_2/g, the S_{BET} for a physical mixture of PAN/SBA- 15 with PAN: SBA-15 wt ratio of 5:1 is expected to be 153 m_2/g in case of 100% accessibility of SBA-15. However, the pore widths of SBA-15, 8 wt% PAN/1.7 wt% SBA-15 and 8 wt% PAN/1.7 wt% SBA-15/0.017 wt% BYK W-9010 are 5.6 nm, 5.4 nm and 5.5 nm, respectively. S_{BET} of nanofiber composites is lower indicating that the porosity of SBA-15 is not totally accessible. For 8wt% PAN/1.7 wt% SBA-15, the S_{BET} of 68.7 m_2/g would indicate that 45% of the porosity is accessible. In the case of 8%wtPAN/1.7 wt% SBA-15/0.017 wt%BYK the S_{BET} is higher with 98.5m_2/g that corresponds to 64% of accessible porosity. The higher pore accessibility may be relied to the deagglomeration effect of the dispersing agent.

FTIR spectrum of (PAN + SBA-15) is shown in Fig. 10 below. The bands of PAN can be assigned as follows: 2941 and 2870 cm^{-1} C-H stretching vibration in C-H_2 stretching vibration of C≡N, 1629 cm^{-1} stretching vibration in C=C, 1452 cm^{-1} bending vibration of C-H_3 and CH_2 groups, 1374 cm^{-1} bending vibration of CH_3 symmetric in CCH_3, 1225 cm^{-1} twisting vibration of C=O. The characteristics bands at 1070, 535 and 458 cm^{-1} are corresponding to the stretching, bending and out of plane of Si–O bonds, respectively. Whereas bands at 939 cm^{-1} is for Si–OH stretching, 1630 cm^{-1} for C-O bending, 2243 cm^{-1} for Si–C stretching [44, 45].

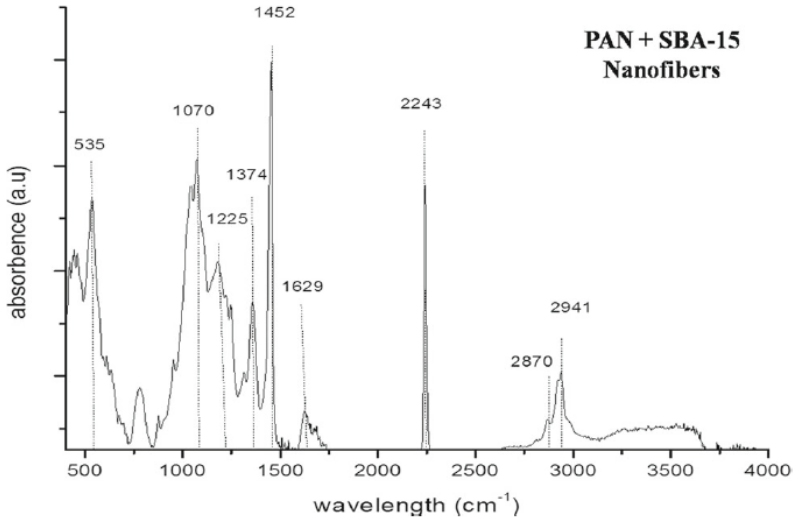

Fig. 10 FTIR spectrum of pure PAN + SBA-15

4 Conclusions

Finding the best parameters for electrospinning is very important for smooth process and continuous manufacturing of nanofibers. PAN concentration, electrode distance, electrode voltage, etc., give significant effect in electrospinning process. In this study, 8wt% of PAN in DMSO at 30 and 50 kV and electrode distance of 12.5 cm were identified as the best parameters for electrospinning of nanofibers. Increase in polymer concentration

gives increase in nanofibers diameter, which is due to higher number of polymer chain entanglements due to high viscosity. Increasing the electrode distance decreases nanofibers diameter due to the long flight of polymer jet. Addition of ordered mesoporous silica particles increased the viscosity of polymer solution and after electrospinning it gave composite nanofibers of larger diameter and high CV%. Among different dispersing agents, BYKW- 9010 was identified as the best choice for deagglomeration of silica particles in the proportion of 1 wt% as compared to silica. It was successfully imparted in nanofibers and led to a better deagglomeration of silica nanoparticles, resulted in a little reduction of nanofibers diameter and related CV%, and reduction of aggregates. Tensile strength of nanofibers was increased by adding silica nanoparticles with or without dispersing agent. The presence of silica particles in the nanofibers structure has also increased the surface area (S_{BET}) since PAN nanofibers are non-porous. Pores coming from the SBA-15 silica particles were found partially blocked and a porosity accessibility of 45% was observed, which could be increased to 64% with dispersing agent.

Research Highlights

- Polyacrylonitrile/mesoporous silica (SBA-15) composites nanofibers were prepared by electrospinning.
- Increase in Surface area by preparing composite of PAN with Silica nanoparticles from 68.7 m_2/g to 98.5 m2/g.
- PAN composite nanofibers also increased thermal stability up to 650° C.
- Polyacrylonitrile/mesoporous silica (SBA-15) composites nanofibers have potential application in energy storage and water purification

Supplementary Information The online version contains supplementary material available at https://doi.org/10.1007/s13369-023-08320-8.

Acknowledgements M.H. Rafe thanks Campus France for his PhD grant. The authors warmly thank Philippe Blondel from LPMT for SEM images and Charles-Henry Deguines from LPIM for rheology, TGA and DLS analyses. Loïc Vidal and Habiba Nouali in charge of Electronic Microscopy and Adsorption platforms of IS2M, respectively, are also gratefully thanked.

Author contribution M.H. Rafe Investigation and writing, original draft preparation K.S. Review & editing, L.J., M.B.: Investigation, E.M.: Data discussion, review, C.D., B.L., D.C.A.: Conceptualization, Methodology, Supervision, review & editing.

Declaration Conflict of interest The authors declare that they have no known competing financial interests or personal relationship that could have appeared to influence the work repeated in this paper.

References

1. Mushtaq, S., et al.: In vitro cytotoxicity of secondary metabolitesextracted from Pseudomonas aeruginosa BS25 strain. Arab. J. Sci.Eng. **45**, 81–94 (2020)
2. Mushtaq, S., et al.: Biocompatibility and cytotoxicity in vitro of surface-functionalized drug-loaded spinel ferrite nanoparticles. Beilstein J. Nanotechnol. **12**(1), 1339–1364 (2021)
3. Mushtaq, S., et al.: Magnetoelectric core–shellCoFe 2O4@BaTiO3 nanorods: their role in drug delivery and effect on multidrug resistance pump activity in vitro. RSC Adv. **12**(38), 24958–24979
(2022)
4. Carvalho, D.V., et al.: High temperature stable separator for lithium batteries based on SiO2 and hydroxypropyl guar gum.Membranes **5**(4), 632–645 (2015)
5. Xu, S., et al.: Design of facile technology for the efficient removal of hydroxypropyl guar gum from fracturing fluid. PLoS ONE **16**(3), e0247948 (2021)
6. Faccini,M., et al.: Electrospun carbon nanofiber membranes for filtration of nanoparticles from water. J.Nanomater. **2015**, 2–2 (2015)
7. Akhtar, S., et al.: Synthesis and characterization of amphotericin B stabilized gold nanoparticles sensor for detection of clindamycin drug. Mater. Res. Exp. **6**(7), 075068 (2019)
8. Shahzad,K., et al.: Effect of Magnesium Substitution on Structural, Magnetic and Biological Activity of Co (1–x)Mg(x) Fe2O4 Nanocolloids. J. Cluster Sci. **32**(4), 1003–1014 (2021)
9. Dai, L., et al.: Properties of hydroxypropyl guar/TEMPO-oxidized cellulose nanofibrils composite films. Cellulose **22**, 3117–3126 (2015)
10. Alghoraibi, I. & Alomari, S.: *Different methods for nanofiber design and fabrication.* Handbook of nanofibers 1–46, (2018)
11. Babu, A., et al.: Ternary structured magnesium cobalt oxide/graphene/polycarbazole nanohybrids for high performance electrochemical supercapacitors. Mater. Sci. Energy Technol. **6**, 399–408 (2023)
12. Almuhamed, S., et al.: Electrospinning of PAN nanofibers incorporatingSBA-15-type ordered mesoporous silica particles. Eur. Polymer J. **54**, 71–78 (2014)

13. Qamar, Z., et al.: Optical,morphological, and impedance characteristics of Ni (x)–(CdO)(1–x) nanofibers fabricated by electrospinning technique. Mater. Sci. Eng. B **282**, 115779 (2022)
14. Yoon, K., et al.: High flux ultrafiltration membranes based on electrospun nanofibrous PAN scaffolds and chitosan coating. Polymer **47**(7), 2434–2441 (2006) 15. Vijayalakshmi,V.; Sadanandan, B.;Anjanapura, R.V.: In vitro comparative cytotoxic assessment of pristine and carboxylic functionalized multiwalled carbon nanotubes on LN18 cells. J. Biochem. Mol. Toxicol. **37**(3), e23283 (2023)
16. Mahesh, R., et al.: Removal of pollutants from wastewater using alumina based nanomaterials:Areview.Korean J. Chem.Eng. 1–11 (2023)
17. Liu, W.; Adanur, S.: Properties of electrospun polyacrylonitrile membranes and chemically-activated carbon nanofibers. Text. Res. J. **80**(2), 124–134 (2010)
18. Atif, M., et al.: Structural, magnetic, and dielectric properties of Ti^{4+}− M^{2+} co-doped $BaFe_{11}Ti_{0.5}M_{0.5}O_{19}$ hexaferrites (M_Co^{2+}, Ni^{2+}, Zn^{2+}). Ceram. Int. **47**(11), 15245–15252 (2021)
19. Sabantina, L., et al.: Investigation of needleless electrospun PAN nanofiber mats. In AIP Conference Proceedings. AIP Publishing LLC (2018)
20. Eom, Y.; Kim, B.C.: Solubility parameter-based analysis of polyacrylonitrile solutions in N N-dimethyl formamide and dimethyl sulfoxide. Polymer **55**(10), 2570–2577 (2014)
21. Kurban,Z., et al.:Turbostratic graphite nanofibres from electrospun solutions of PAN in dimethylsulphoxide. Eur. Polymer J. **46**(6), 1194–1202 (2010)
22. Liao, C., et al.: Synthesis and characterization of SBA-15/poly (vinylidene fluoride) (PVDF) hybrid membrane. Desalination **260**(1–3), 147–152 (2010)
23. Shahzad, K., et al.: Effect of lanthanum substitution on shape and cytotoxicity of zinc oxide (La_xZn_{1-} XO) nano-colloids. Mater.Res. Exp. **6**(5), 055012 (2019)
24. Shahzad, K., et al.: Field-controlled magnetoelectric core-shell
$CoFe_2O_4$@ $BaTiO_3$ nanoparticles as effective drug carriers and drug release in vitro. Mater. Sci. Eng. C **119**, 111444 (2021)
25. Akhtar, S., et al.: Antibacterial and antiviral potential of colloidalTitanium dioxide (TiO_2) nanoparticles suitable for biological applications. Mater. Res. Exp. **6**(10), 105409 (2019)
26. Vysko˘cilová, E., et al.: Modified MCM-41 as a drug delivery system for acetylsalicylic acid. Solid State Sci. **38**, 85–89 (2014)
27. Almuhamed, S.: Study and development of nonwovens made of electrospun composite nanofibers, Mulhouse (2015)
28. Dang, Y.T., et al.: Microwave-assisted synthesis of nano Hf-and Zr-based metal-organic frameworks for enhancement of curcumin adsorption. Microporous Mesoporous Mater. **298**, 110064 (2020)
29. Brauneur, S.; Emmet, P.; Teller, E.: Adsorption of gases in multi molecular layer. J. Am. Chem. Soc. **60**, 309–319 (1938)
30. Broekhoff, J., & De Boer J.: Studies on pore systems in catalysts: IX. Calculation of pore distributions from the adsorption branch of nitrogen sorption isotherms in the case of open cylindrical pores A. Fundamental equations. J. Catal. **9**(1): 8–14 (1967)
31. McKee, M.G.;Wilkes, G.L.; Colby, R.H.; Long, T.E.: Correlations of solution rheology with electrospun fiber formation of linear and branched polyesters. Macromolecules **37**(5), 1760–1767 (2004)
32. Cook, A.G., et al.: Synthesis and phase behaviour of a homologous series of polymethacrylate-based side-chain liquid crystal polymers. Eur. Polymer J. **48**(4), 821–829 (2012)
33. Pilehrood, M.K.; Heikkilä, P.; Harlin, A.: Preparation of carbon nanotube embedded in polyacrylonitrile (pan) nanofibre composites by electrospinning process. AUTEX Res. J. **12**(1), 1–6 (2012)
34. Jalili, R.; HOSSEINI, S. A. A.; Morshed,M.: The effects of operatingparameters on the morphology of electrospun polyacrilonitrile nanofibers (2005)
35. Beachley, V.;Wen, X.: Effect of electrospinning parameters on thenanofiber diameter and length. Mater. Sci. Eng. C **29**(3), 663–668 (2009)
36. Nazir, A.: Modelling and optimization of electrospun materials for technical applications. Université de Haute Alsace-Mulhouse; National Textile University (Pakistan) (2016)
37. Rafe,M.H.: Advanced electrospun composite for wastewater treatment. PhD thesis, Université de Haute-Alsace, Mulhouse, France (2021)
38. Grassie, N.; McGuchan, R.: Pyrolysis of polyacrylonitrile and related polymers—I. Thermal analysis of polyacrylonitrile. Eur. Poly. J. **6**(9), 1277–1291 (1970)
39. Goracheva,V., et al.: Thermographic and thermogravimetric analysis of the thermal behaviour of polyacrylonitrile fibres. Fibre Chem. **5**(5), 496–498 (1974)
40. Xiao, S., et al.: Thermal behavior and kinetics during the stabilization of polyacrylonitrile precursor in inert gas. J. Appl. Polym. Sci. **122**(1), 480–488 (2011)
41. Xue, T.J.; McKinney, M.A.; Wilkie, C.A.: The thermal degradation of polyacrylonitrile. Polym. Degrad. Stabil. **58**(1–2), 193–202 (1997)
42. Ouyang, Q., et al.:Mechanism and kinetics of the stabilization reactions of itaconic acid-modified polyacrylonitrile. Polym. Degrad. Stab. **93**(8), 1415–1421 (2008)
43. Thommes, M., et al.: Physisorption of gases, with special reference to the evaluation of surface area and pore size distribution (IUPAC Technical Report). Pure Appl. Chem. **87**(9–10), 1051–1069 (2015)
44. Jawalkar, S.S., et al.: Molecular dynamics simulations on the blendsof poly (vinyl pyrrolidone) and poly (bisphenol-A-ether sulfone). J. Appl. Polym. Sci. **108**(6), 3572–3576 (2008)
45. Ji, L.; Zhang, X.:Ultrafine polyacrylonitrile/silica composite fibers via electrospinning. Mater. Lett. **62**(14), 2161–2164 (2008)